

Nonequilibrium Dephasing in an Electronic Mach-Zehnder Interferometer

Seok-Chan Youn,¹ Hyun-Woo Lee,² and H.-S. Sim^{1,*}

¹*Department of Physics, Korea Advanced Institute of Science and Technology, Daejeon 305-701, Korea*

²*PCTP and Department of Physics, Pohang University of Science and Technology, Pohang, Kyungbuk 790-784, Korea*

(Dated: August 16, 2021)

We study nonequilibrium dephasing in an electronic Mach-Zehnder interferometer. We demonstrate that the shot noise at the beam splitter of the interferometer generates an ensemble of nonequilibrium electron density configurations and that electron interactions induce configuration-specific phase shifts of an interfering electron. The resulting dephasing exhibits two characteristic features, a lobe pattern in the visibility and phase jumps of π , in good agreement with experimental data.

PACS numbers: 85.35.Ds, 72.70.+m, 03.65.Yz, 73.23.-b

Introduction. — An electronic analog of optical Mach-Zehnder interferometry (E-MZI) has been recently realized [1, 2, 3, 4] by utilizing edge channels of integer quantum Hall (IQH) liquids. As it is one of elementary types of interferometry, it can serve as an important probe of electronic coherence [5] and entanglement [6, 7, 8].

The E-MZI has a simple setup consisting of two arms and two beam splitters. Recent experiments [2, 4] on it, nevertheless, revealed puzzling behavior that is hard to understand within a noninteracting-electron description [9]; the interference visibility of the differential conductance shows bias-dependent lobe patterns, accompanied by phase jumps of π at the minima of the lobes. There may exist some unnoticed fundamental physics behind it.

Electron-electron interactions may be important for the puzzling nonequilibrium behavior. Interaction effects were studied [10, 11] in the tunneling regime by using bosonization methods. In Ref. [10], interactions between an E-MZI channel and an additional one outside the E-MZI were considered and the resulting resonant plasmon excitations were proposed as an origin of the puzzle. On the other hand, roles of the shot noise of an additional detecting channel were addressed [12, 13] to understand similar lobes found in a related experiment [12].

In this work, we propose an intrinsic mechanism for the puzzling behavior, which does not require additional channels outside the E-MZI. A key observation is that the shot noise at the input beam splitter of the E-MZI generates an *ensemble of nonequilibrium electron density configurations* in the two arms. Then the electron interaction *within each arm* induces configuration-specific phase shifts of an interfering electron, and the ensemble average of the phase shifts leads to nonequilibrium dephasing. The combined effect of the shot noise and the interaction results in lobe patterns and phase jumps, which agree with experimental data [2, 4]. We use a *wave-packet* picture to describe the nonequilibrium density and treat the interaction phenomenologically at zero temperature. The inter-arm interaction is ignored.

E-MZI setup — The E-MZI consists of two sources $i = 1, 2$, two drains $i = 3, 4$, two beam splitters $j = a, b$, and two arms $l = u, d$ of length L_l [Fig. 1(a)]. The

source $i = 1$ is biased by $|e|V$, while $i = 2$ is unbiased. Transmission probabilities at the splitter j are T_j and $R_j (= 1 - T_j)$. Each arm consists of a single edge channel of the IQH liquid with the linear energy dispersion characterized by constant group velocity v_F . We first consider the simple case with $L_u = L_d \equiv L$, and later discuss the case with $L_u \neq L_d$. There are two time scales, electron flight time $t_{\text{fl}} \equiv L/v_F$ through an arm and time separation $\tau_V = 2\pi\hbar/(|e|V)$ between successive injections of *nonequilibrium* electrons (with single-particle energy $\in [0, |e|V]$) from the source 1. Their ratio gives the average number of the nonequilibrium electrons in the two arms at a given time,

$$N = \frac{t_{\text{fl}}}{\tau_V} = \frac{L|e|V}{2\pi\hbar v_F}. \quad (1)$$

Nonequilibrium density configurations. — At zero temperature, the nonequilibrium state of the E-MZI can have

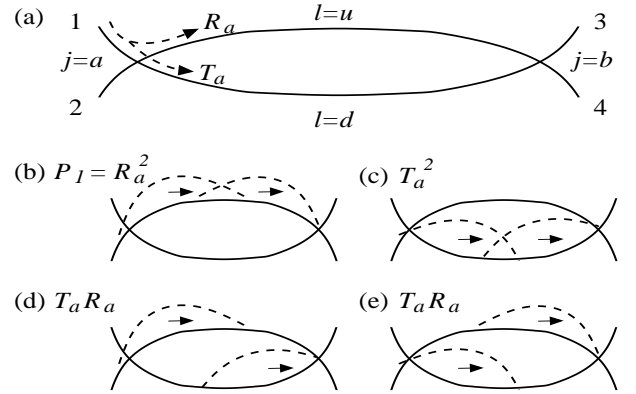


FIG. 1: (a) Schematic E-MZI setup. It has two beam splitters $j = a, b$ with transmission probabilities T_j and R_j , two arms $l = u, d$, two sources $i = 1, 2$, and two drains $i = 3, 4$. Only the source 1 is biased. (b-e) Schematic nonequilibrium ensemble of electron density configurations in the two arms resulting from the shot noise at the splitter a when the two arms have two nonequilibrium electrons. The configurations can be described by two packets (dashed lines) propagating towards the drains as marked by solid arrows. The probability P_m of each ensemble element m is marked.

the two equivalent forms in the noninteracting limit,

$$|\Psi(t)\rangle_{\text{nint}} = \hat{U}(t) \prod_{E=0}^{|e|V} c^\dagger(E)|0\rangle = \hat{U}(t) \prod_{n=-\infty}^{\infty} d^\dagger(nW)|0\rangle, \quad (2)$$

where $\hat{U}(t)$ is the time evolution operator, $|0\rangle$ is the Fermi sea in equilibrium, and $c^\dagger(E)$ creates an electron with the single-particle energy E in the scattering wave $\psi(E)$ incoming from the source 1. $d^\dagger(X = nW)$ creates an electron in the wave packet [14, 15], $\phi(X) \propto \int_0^{|e|V} dE \exp(-iEX/\hbar v_F) \psi(E)$, centered at position $x = X$ with packet width $W = v_F \tau_V$. Here, n is an integer and we use the convention that both the arms amount to the range $(-L/2, L/2)$. Thus for $-L/2 < X < L/2$, the packet center is located in the arm u or d . The equivalence between the two forms in Eq. (2) can be easily verified from the identity $\{d(nW), d^\dagger(n'W)\} = \delta_{n,n'}$ and the Pauli exclusion. While the former form is more commonly used, e.g., in the linear response regime, the latter may provide more insightful understanding of the ensemble of nonequilibrium electron density configurations and the resulting intrinsic dephasing mechanism, as shown below. Later we use a combination of the two forms.

As time t passes, $\phi(X)$ evolves to $\phi(X + v_F t)$. When a packet arrives at the input splitter a , it propagates into the arm u with the probability R_a or into the arm d with T_a . This process describes the shot noise [14, 16] and generates a nonequilibrium ensemble of electron density configurations in the arms. The ensemble depends on N , i.e., on how many packets have significant weight in the arms. For example, for $N \ll 1$, only one packet has significant weight and the ensemble has two representative elements $m = 1, 2$, in each of which the nonequilibrium density appears in the arm u (d) with probability $P_{m=1} = R_a$ ($P_{m=2} = T_a$) at any given time. In this case, the nonequilibrium state has the form of $|\Psi\rangle_{\text{nint}} = \sum_{m=1,2} c_m |\Psi_m\rangle_{\text{nint}}$ where $|c_m|^2 = P_m$ and $|\Psi_{m=1(2)}\rangle_{\text{nint}}$ contains the packet state with significant weight in the arm u (d) and no weight in d (u). Similarly, when two packets have considerable weight [Figs. 1(b-e)], the ensemble has four representative elements $m = 1, 2, 3, 4$, with probability $P_m = R_a^2, T_a^2, T_a R_a$, and $R_a T_a$, respectively. When the interaction is turned on, each density configuration causes different phase shift to an interfering electron, resulting in the nonequilibrium dephasing.

Lobe patterns in transmission probability. — We focus on a weak-interaction regime where the energy relaxation rate is sufficiently smaller than t_{tr}^{-1} [5]. In this regime, a single-particle energy E_0 ($\in [0, |e|V]$) is a well defined quantity, and thus one can consider the interference of the scattering plane wave $|\psi(E_0)\rangle$. Within the arms, $|\psi(E_0)\rangle$ shows the superposition, $|\psi(E_0)\rangle = r|u(E_0)\rangle + t|d(E_0)\rangle$, of the plane waves $|l(E_0)\rangle$ in the arms $l = u, d$, where $|r|^2 = R_a$ and $|t|^2 = T_a$. The phase accumulation of $|l(E_0)\rangle$ is affected by the interaction between $|\psi(E_0)\rangle$ and

the rest of the nonequilibrium electrons. We call the rest as the environment of the electron in $|\psi(E_0)\rangle$.

To see how the interaction affects the phase accumulation, we write the total nonequilibrium state as $|\Psi\rangle = |\Psi\rangle_{\text{nint}} = |\psi(E_0)\rangle \otimes |\Phi_{E_0}\rangle$. We will later turn on a weak interaction between $\psi(E_0)$ and Φ_{E_0} , and ignore the interaction among the environment electrons, as a weak interaction may only slightly modify the nonequilibrium densities from the noninteracting case. Both $\psi(E_0)$ and the environment electrons in Φ_{E_0} are injected from the source 1 and end in either the drain 3 or 4. As Φ_{E_0} will be traced out to obtain the transmission probability $\mathcal{T}(E_0)$ of $\psi(E_0)$ to a drain, one has freedom of choosing either the wave-packet or the plane-wave description for Φ_{E_0} . We choose the former, since it is more insightful and convenient for obtaining the density configurations of Φ_{E_0} in the arms, which is essential to describe the interaction. In the former, Φ_{E_0} is described by the moving train of wave packets constructed by single-particle states with energy $\in [0, |e|V]$ except E_0 ; the exclusion of E_0 negligibly modifies the packets from $\phi(X)$. As discussed before, due to the shot noise at the splitter $j = a$, $|\Phi_{E_0}\rangle$ has the superposition, $|\Phi_{E_0}\rangle = \sum_m c_m |\Phi_{E_0,m}\rangle$, of the multiple-packet states, each corresponding to an element m (with $P_m = |c_m|^2$) of the nonequilibrium density ensemble. As the spatial configurations of the moving packets are repeated in time with periodicity τ_V , time ensemble average over $[0, \tau_V]$, in addition to the average over the nonequilibrium density ensemble, is necessary to obtain $\mathcal{T}(E_0)$. We remark that the ensemble averages cannot be captured by a mean-field approach.

We turn on a weak interaction between $\psi(E_0)$ and Φ_{E_0} . It causes the phase shift of Ψ described by an operator, $\hat{U}_{\text{ph}}(t_0) = \sum_{l=u,d} e^{-i\frac{U_0}{\hbar} \int_{t_0}^{t_0+t_n} dt \hat{N}_l(t)} |l(E_0)\rangle \langle l(E_0)|$. Here, U_0 is the interaction strength (assumed [17] to be independent of $|e|V$), $t_0 \in [0, \tau_V]$ is the time-ensemble index, and $\hat{N}_l(t) = \int_{x \in l} \hat{n}(x, t) dx$ acts on $|\Phi_{E_0}\rangle$ to measure the number of the environment electrons in arm l at time t . The time ordering operator is dropped in \hat{U}_{ph} as the packet dynamics $\phi(X + v_F t)$ makes $[\hat{N}_l(t), \hat{N}_{l'}(t')]$ a c -number [13].

The interference signal of the interfering electron with energy E_0 can be obtained from the reduced density matrix $\text{Tr}_{\text{env}}[\hat{U}_{\text{ph}}(t_0)|\Psi\rangle \langle \Psi| \hat{U}_{\text{ph}}^\dagger(t_0)]$, which is found to be

$$R_a |u(E_0)\rangle \langle u(E_0)| + T_a |d(E_0)\rangle \langle d(E_0)| + \sum_m P_m (r t^* \langle e^{i\hat{\delta}(t_0)} \rangle_m |u(E_0)\rangle \langle d(E_0)| + \text{h.c.}), \quad (3)$$

where $e^{i\hat{\delta}} \equiv e^{-i\frac{U_0}{\hbar} \int_{t_0}^{t_0+t_n} dt [\hat{N}_u(t) - \hat{N}_d(t)]}$ and $\langle \dots \rangle_m \equiv \langle \Phi_{E_0,m} | \dots | \Phi_{E_0,m} \rangle$. The trace Tr_{env} over all the orthogonal multiparticle states $\{|\Phi_{\text{env},i}\rangle\}$ of the environment electrons is evaluated using the fact that $|\Phi_{E_0,m}\rangle$ and $|\Phi_{E_0,m' \neq m}\rangle$ are “severely” orthogonal to each other, i.e., $\langle \Phi_{\text{env},i} | \prod_{k=1}^{k_{\text{max}}} \hat{n}(x_k) | \Phi_{E_0,m} \rangle \langle \Phi_{E_0,m'} | \prod_{k'=1}^{k'_{\text{max}}} \hat{n}(x_{k'}) | \Phi_{\text{env},i} \rangle$

is nonzero only for $m = m'$ where $k_{\text{mx}}, k'_{\text{mx}}$ are finite positive integers; any finite number of local density operators can not transform a packet of finite width into another orthogonal packet. The off-diagonal part of the reduced density matrix in Eq. (3) describes the dephasing of $|\psi(E_0)\rangle$ due to the interaction.

The factor $\langle e^{i\hat{\delta}} \rangle_m$ can be further evaluated as

$$\langle e^{i\hat{\delta}(t_0)} \rangle_m \simeq e^{i\langle \hat{\delta}(t_0) \rangle_m} = e^{-i\frac{U_0}{\hbar} \int_{t_0}^{t_0+t_{\text{fl}}} dt \langle \Delta \hat{N}(t) \rangle_m}, \quad (4)$$

where $\Delta \hat{N}(t) \equiv \hat{N}_u(t) - \hat{N}_d(t)$. In Eq. (4), we ignore the number fluctuation, $\langle \Delta \hat{N}(t) \Delta \hat{N}(t') \rangle_m - \langle \Delta \hat{N}(t) \rangle_m \langle \Delta \hat{N}(t') \rangle_m$, or $\langle \hat{\delta}(t_0) \hat{\delta}(t_0) \rangle_m - \langle \hat{\delta}(t_0) \rangle_m^2$, based on the observation that it is not a crucial factor for the nonequilibrium dephasing [18].

From Eq. (3), the transmission probability of the electron in $\psi(E_0)$ to the drain $i = 3$ is obtained as

$$\mathcal{T} \equiv \mathcal{T}(E_0) = \mathcal{T}_0 + \mathcal{T}_1 D \cos(\Phi_B + \eta_D), \quad (5)$$

where $\mathcal{T}_0 = T_a T_b + R_a R_b$, $\mathcal{T}_1 = 2\sqrt{T_a T_b R_a R_b}$, Φ_B is the Aharonov-Bohm phase, $D \cos(\Phi_B + \eta_D) \equiv \langle \Re[e^{i\Phi_B} \sum_m P_m \langle e^{i\hat{\delta}(t_0)} \rangle_m] \rangle_{t_0}$, $\langle \dots \rangle_{t_0}$ means the ensemble average over time $t_0 \in [0, \tau_V]$, D is the nonequilibrium dephasing factor, and η_D is the phase shift of \mathcal{T} . Notice that \mathcal{T} is independent of E_0 when $L_u = L_d$ and that Eq. (5) reproduces the noninteracting result when $U_0 = 0$.

We first consider the regime of $N \ll 1$ and $U_0 t_{\text{fl}}/\hbar \gg 1$. Though this parameter regime is unphysical [17], it is nevertheless illustrative since it allows the analytic evaluation of D and η_D . In this regime, the packet ϕ may be approximated as a square packet of extension W with constant density of $1/W$, and the nonequilibrium density ensemble has two representative elements, one packet partially in the $l = u$ arm with $P_{m=1} = R_a$ or in d with $P_2 = T_a$, as discussed before. Then, $\langle \hat{\delta}(t_0) \rangle_m$ in Eq. (4) has the constant value of $(-1)^m \delta$,

$$\delta \equiv N \frac{U_0 t_{\text{fl}}}{\hbar} = \frac{|e|V t_{\text{fl}}}{2\pi\hbar} \frac{U_0 t_{\text{fl}}}{\hbar}, \quad (6)$$

and one finds, using $\text{Arg}[\cdot] \equiv \arctan(\text{Im} \cdot / \text{Re} \cdot)$,

$$D = \sqrt{\cos^2 \delta + (R_a - T_a)^2 \sin^2 \delta}, \quad (7)$$

$$\eta_D = \text{Arg}[\cos \delta - i(R_a - T_a) \sin \delta]. \quad (8)$$

Notice that δ is proportional to the bias V and that $D(\delta)$ (thus \mathcal{T}) shows *lobe patterns* with periodic minima of value $|R_a - T_a|$ at $\delta = \pi/2, 3\pi/2, \dots$ [Fig. 2(a)]. The minimum value increases from zero as T_a deviates from 0.5. And, the minima are accompanied by *phase jumps*. At $T_a = 0.5$, η_D shows sharp jumps of π at the minima, while it is zero or π otherwise. The jumps become smeared as T_a deviates from 0.5. All these features are related to the which-path information [19] of the nonequilibrium electrons. As $|e|V$ increases, the phase shift $\langle \hat{\delta} \rangle$

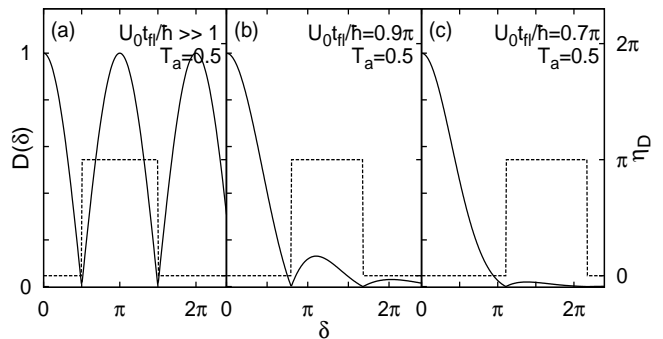


FIG. 2: Nonequilibrium dephasing factor $D(\delta)$ (solid curves) and phase shift $\eta_D(\delta)$ of \mathcal{T} (dashed). In (a), we plot Eqs. (7,8), while (b) and (c) show the numerical results; see text. In (b), N varies from 0 to 2 as δ increases up to 1.8π .

increases (decreases) by δ with probability T_a (R_a) as the environment electrons are in arm d (u). At $T_a = 0.5$, the two possible phase shifts in the opposite direction are balanced in probability, resulting in the sharp jumps in η_D at the lobe minima. When $T_a \neq 0.5$, the balance is broken, leading to the smearing of the jump.

Hereafter, we discuss numerical results for the weak interaction regime with $U_0 t_{\text{fl}}/\hbar < \pi$ [17]. A quantitative calculation needs to take account of a larger number of nonequilibrium ensemble elements than Fig. 1 might imply, since the packet ϕ has a rather slowly decaying tail and more importantly for given N , about $2N$ packets appear in the arms during t_{fl} . Thus the minimum number of ensemble elements for a given N is 2^{2N} ; in the calculation, 2^9 elements are considered in the regime of $N \leq 3$. Such variety (of $\langle e^{i\hat{\delta}(t_0)} \rangle_m$) modifies the lobes [Figs. 2(b,c)]. Interestingly, the lobes in D and the jumps in η_D of the $N \ll 1$ case are maintained, though the lobes now acquire a decaying envelope and the minimum positions of the lobes are shifted. This robustness can be understood as follows. Among the 2^{2N} elements of the nonequilibrium density ensemble, those with probability $P_m = R_a^{2N}$ or T_a^{2N} have $\langle \Delta \hat{N} \rangle_m = N$ or $-N$, generating the same phase shift of $\pm\delta$ at all t_0 's as in the $N \ll 1$ case, while in the others $\langle \Delta \hat{N} \rangle_m$ varies with t_0 within a range smaller than δ . After the ensemble average over t_0 , the lobes themselves survive due to the former, while the latter has less contribution to \mathcal{T} , giving rise to the decaying envelope and the shift of the lobe positions. For smaller $U_0 t_{\text{fl}}/\hbar$, larger number of packets are involved (at a given δ), resulting in more rapidly decaying envelope and thus smaller number of visible lobes [Fig. 2(c)].

Lobe patterns in dI/dV . — From the zero-temperature current $I = (|e|/\hbar) \int_0^{|e|V} dE_0 \mathcal{T}(E_0) = (e^2/\hbar) V \mathcal{T}$, one evaluates $dI/dV = (e^2/\hbar) \mathcal{T}_0 [1 + F(V) \cos(\Phi_B + \eta_F(V))]$. Here, $F(V)$ gives the visibility of dI/dV , $(dI/dV|_{\text{max}} - dI/dV|_{\text{min}})/(dI/dV|_{\text{max}} + dI/dV|_{\text{min}})$, and η_F is the phase shift of dI/dV ; remember $\delta \propto V$ and $L_u = L_d$.

The lobes in \mathcal{T} give rise to similar lobes in dI/dV .

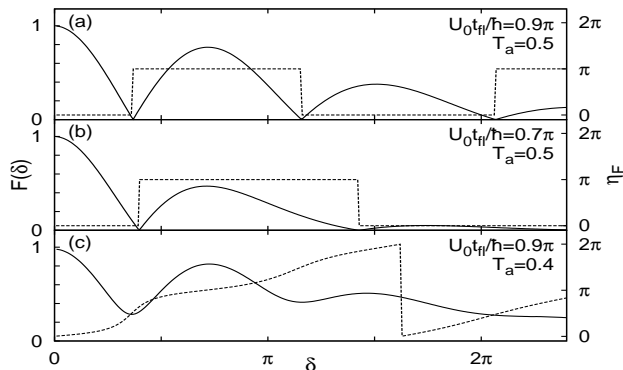


FIG. 3: Visibility F (solid curves) and phase shift η_F (dashed) of dI/dV , as a function of δ .

At $T_a = 0.5$, the visibility $F(V)$ shows a lobe pattern whose minima reach zero and the phase η_F jumps by π at the minima of the lobes while staying constant in other regions. The number of visible lobes in $F(V)$ becomes smaller for smaller $U_0 t_F / \hbar$, similar to D [Figs. 3(a,b)]. The first zero of $F(V)$ appears even for small $U_0 t_F / \hbar$ where the second lobe of \mathcal{T} almost vanishes [Figs. 2(c) and 3(b)]. As T_a deviates from 0.5, the minimum values of $F(V)$ increase from zero, similarly to those of D , and the jumps of η_F become smeared. In this case the jump around the first minimum of $F(V)$ is sharper than that around the second [Fig. 3(c)].

Discussion. — The lobes and phase jumps in Fig. 3 qualitatively agree with the experimental data [2, 4] at $T_a = 0.5$, where $N \simeq 0.4 - 1$ at $V = 8 \mu\text{V}$ in the E-MZI with $L \simeq 10 \mu\text{m}$ and $v_F \simeq (2-5)10^4 \text{ m/s}$. The first minimum of $F(V)$ occurs around $\delta \simeq 3\pi/8$ (where $N \simeq 0.4$) in Fig. 3, while around $V = 8 \mu\text{V}$ in the data. From this, we estimate $U_0 \simeq 1.5 - 9 \mu\text{eV}$ for the experimental E-MZIs. The dependence of the number of visible lobes in $F(V)$ on $U_0 t_F / \hbar$ [17] indicates that the number depends on the magnetic field, disorder, equilibrium electron density, etc, as in the data. Note that the minima of $F(V)$ look periodic in V in Fig. 3(a), although not in general.

The case with $\Delta L \equiv L_u - L_d \neq 0$ can be understood from Eqs. (5,7,8). D and η_D have the same forms as in Eqs. (7,8) except for the replacements, $\delta \rightarrow \alpha V(L_u + L_d)/2$ and $\eta_D \rightarrow \eta_D + E_0 \Delta L / \hbar v_F - \alpha V \Delta L / 2$, where $\alpha = |e|U_0 t_F / (2\pi \hbar^2 v_F)$. Then, the shift of the lobe-minimum positions is governed by $(L_u + L_d)/2$, and for $U_0 t_F / \hbar < \pi$, η_F becomes an undulating function that no longer shows sharp jumps. These modifications are however negligible for $\Delta L \ll W = 2\pi \hbar v_F / (|e|V)$, in agreement with experimental data [2].

We suggest that the combined experimental analysis of both I and dI/dV may be useful since I can provide the direct information of the dephasing factor D . And, our formalism may be applicable to possible nonequilibrium dephasing in other electronic interferometries [12]. Finally, careful treatment of the number fluctuation [18], ignored in Eq. (4), may give further understanding, as it

may modify the decaying envelope and the lobe positions.

In summary, we have shown that the nonequilibrium density ensemble, generated by the shot noise at the input beam splitter, can cause the nonequilibrium dephasing in the E-MZI. Our result suggests that the experimental data in Ref. [2] may only be the first of its kind with more nonequilibrium quantum effects waiting for their discoveries.

We thank I. Neder for sending us experimental data and M. Büttiker for useful discussions. We are supported by KRF (2006-331-C00118, 2005-070-C00055) and by MOST through the leading basic S & T research projects.

Note added.— During our manuscript preparation, a preprint [20] addressing shot-noise effects in the E-MZI was reported. It considers a regime of the interaction strength stronger than ours.

* Electronic address: hssim@kaist.ac.kr

- [1] Y. Ji *et al.*, Nature **422**, 415 (2003).
- [2] I. Neder *et al.*, Phys. Rev. Lett. **96**, 016804 (2006).
- [3] L. V. Litvin *et al.*, Phys. Rev. B **75**, 033315 (2007).
- [4] P. Roulleau *et al.*, Phys. Rev. B **76**, 161309(R) (2007).
- [5] P. Roulleau *et al.*, Phys. Rev. Lett. **100**, 126802 (2008).
- [6] P. Samuelsson, E. V. Sukhorukov, and M. Büttiker, Phys. Rev. Lett. **92**, 026805 (2004).
- [7] H.-S. Sim and E. V. Sukhorukov, Phys. Rev. Lett. **96**, 020407 (2006).
- [8] I. Neder *et al.*, Nature **448**, 333 (2007).
- [9] See, e.g., V. S.-W. Chung, P. Samuelsson, and M. Büttiker, Phys. Rev. B **72**, 125320 (2005).
- [10] E. V. Sukhorukov and V. V. Cheianov, Phys. Rev. Lett. **99**, 156801 (2007).
- [11] J. T. Chalker, Y. Gefen, M. Y. Veillette, Phys. Rev. B **76**, 085320 (2007).
- [12] I. Neder *et al.*, Nature Physics **3**, 534 (2007).
- [13] I. Neder and F. Marquardt, New J. Phys. **9**, 1 (2007).
- [14] Th. Martin and R. Landauer, Phys. Rev. B **45**, 1742 (1992).
- [15] In an infinite one-dimensional wire, one finds $\phi(X) = (e^{if(x)}/\sqrt{W}) \sin[f(x)]/f(x)$, where $f(x) = \pi(x - X)/W$.
- [16] M. Büttiker, Phys. Rev. Lett. **65**, 2901 (1990).
- [17] One may have $U_0 \sim e^2/(\epsilon L)$, where ϵ is the dielectric constant of the arms. Then, $U_0 t_F / \hbar \sim e^2/(\epsilon \hbar v_F)$ is independent of $|e|V$ and L , justifying our assumption of U_0 being independent of V . And, we choose $U_0 t_F / \hbar < \pi$, where single-particle level spacing $\hbar\pi/t_F$ is larger than U_0 so that the E-MZI is in the weak interaction regime.
- [18] When $\hat{N}_I(t)$ is projected onto the energy window $[0, |e|V]$, the number fluctuation is indeed negligible. Even when the virtual transition to outside this energy window caused by $\hat{N}_I(t)$ is taken into account, it may not affect the lobe pattern qualitatively since the m -dependence of this fluctuation is negligible, though it may modify the decaying envelope and the lobe minimum positions.
- [19] R. P. Feynmann, R. B. Leighton, and M. Sands, *The Feynmann Lectures on Physics III* (Addison-Wesley, 1989).
- [20] I. Neder and E. Ginossar, cond-mat/0711.1293.